

## The organization of divalent cations in the active site of cadmium *Escherichia coli* fructose-1,6-bisphosphate aldolase

David R. Hall,<sup>a†</sup> Lauris E. Kemp,<sup>a</sup>  
 Gordon A. Leonard,<sup>b</sup> Karen  
 Marshall,<sup>c</sup> Alan Berry<sup>d</sup> and  
 William N. Hunter<sup>a\*</sup>

<sup>a</sup>Division of Biological Chemistry and Molecular Microbiology, School of Life Sciences, University of Dundee, Dundee DD1 5EH, Scotland, <sup>b</sup>Joint Structural Biology Group, ESRF, BP220, F38043 Grenoble CEDEX, France, <sup>c</sup>Department of Biochemistry, University of Cambridge, Tennis Court Road, Cambridge CB2 1QW, England, and <sup>d</sup>School of Biochemistry and Molecular Biology, University of Leeds, Leeds LS2 9JT, England

† Current address: Molecular Enzymology Group, Clare Hall Laboratories, Cancer Research UK, South Mimms, Hertfordshire EN6 3LD, England.

Correspondence e-mail:  
 w.n.hunter@dundee.ac.uk

Previously determined crystal structures of the zinc enzyme *Escherichia coli* class II fructose-1,6-bisphosphate aldolase display good agreement for the protein structure but a differing metal-ion organization in the active site. The structure of the enzyme with Cd<sup>2+</sup> in place of Zn<sup>2+</sup> has now been determined to 2.0 Å resolution to facilitate cation identification. The protein structure was essentially identical to other structures and five Cd<sup>2+</sup> positions were identified. Two of the cations are at the active site; one corresponds to the catalytic ion and the other provides a structural contribution. These Cd<sup>2+</sup> sites are equivalent to two Zn<sup>2+</sup> ions observed when the enzyme is complexed with a transition-state mimic and confirm our assignment of the roles played by these ions.

Received 21 August 2002  
 Accepted 23 December 2002

**PDB Reference:** cadmium fructose-1,6-bisphosphate aldolase, 1gyn, r1gynsf.

### 1. Introduction

Fructose-1,6-bisphosphate aldolase (FBPA; EC 4.1.2.13) catalyses the condensation of dihydroxyacetone phosphate (DHAP) with glyceraldehyde 3-phosphate (G3P) to form fructose 1,6-bisphosphate (FBP; Gefflaut *et al.*, 1995; Horecker *et al.*, 1972) in gluconeogenesis and the reverse reaction in glycolysis. These aldolases catalyse the formation of C—C bonds with exquisite stereochemical control and offer new opportunities in biotransformation chemistry. The metal-dependent or class II aldolases have attracted attention as they are more stable than the class I enzymes, which utilize an active-site lysine in Schiff-base formation.

Class II FBPA has an absolute requirement for a divalent cation, usually Zn<sup>2+</sup>, and is activated by monovalent cations (Horecker *et al.*, 1972). Independent structure determinations of the *Escherichia coli* enzyme (Zn-FBPA) crystallized under different conditions (Blom *et al.*, 1996; Cooper *et al.*, 1996) showed a dimer of (α/β)<sub>8</sub>-barrels with an active site at the carboxyl side of the barrel. Whilst there was a high level of agreement in the protein structures, there were significant differences with respect to metal-ion positions and coordination (Fig. 1). The high-resolution (1.6 Å) monoclinic structure (Blom *et al.*, 1996) showed two mutually exclusive Zn<sup>2+</sup>-binding sites 3.2 Å apart (termed Zn<sub>s</sub> and Zn<sub>b</sub> for the surface and buried sites, respectively). The

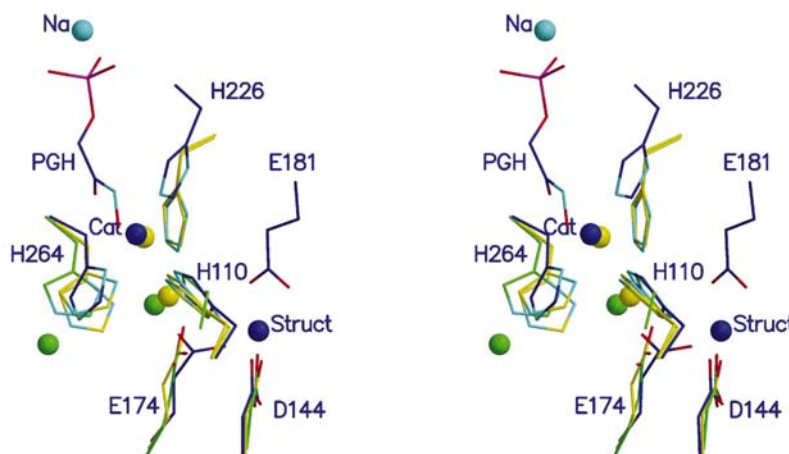


**Figure 1**

Overlaid metal-binding sites of monoclinic and hexagonal Zn-FBPA together with FBPA-PGH. N, O and P atoms are coloured cyan, red and purple, respectively. In monoclinic Zn-FBPA the mutually exclusive Zn<sub>s</sub> and Zn<sub>b</sub> are shown as yellow spheres and the hexagonal Zn-FBPA M1, M2 and C atoms are shown in green. The catalytic (Cat) and structural (Struct) Zn<sup>2+</sup> and ligands of FBPA-PGH are shown in blue and the activating Na<sup>+</sup> is in cyan. Figures were generated with *MOLSCRIPT* (Kraulis, 1991) and *RASTER3D* (Merritt & Murphy, 1994).

cations were assigned occupancies of approximately 0.5 and the two positions were mediated by side-chain rotations of coordinating histidine residues (His110 and His264). A medium-resolution (2.5 Å) structure of a hexagonal form crystallized in the presence of 2 mM ZnCl<sub>2</sub> identified two cation positions (M1 and M2) separated by 6.2 Å, forming a bimetallic active site (Cooper *et al.*, 1996). A site (M2) corresponding to Zn<sub>b</sub> in the monoclinic form was assigned to Zn<sup>2+</sup>. Although refined as K<sup>+</sup>, doubts remained about the true nature of M1, which occupied a site equivalent to that of NH<sub>4</sub><sup>+</sup> in the monoclinic crystal form (not shown). The 2.0 Å structure of FBPA complexed with the DHAP analogue phosphoglycolohydroxamate (PGH) in a trigonal crystal form followed (Hall *et al.*, 1999) and proved to be particularly valuable. The complex revealed aspects of enzyme–ligand interactions relevant to catalysis and was consistent with biochemical and site-directed mutagenesis studies (Plater *et al.*, 1999). The catalytic Zn<sup>2+</sup> was identified and corresponds to the partially ordered Zn<sub>s</sub> of the monoclinic form. There was no Zn<sub>b</sub> equivalent, but there was a second Zn<sup>2+</sup> bound nearby contributing to the organization of the active site (Fig. 1). The buried monovalent cation site assigned in both the monoclinic and hexagonal crystal forms was identified as a well ordered water molecule in the FBPA–PGH complex and a different monovalent binding site was identified, occupied by Na<sup>+</sup>. This ion, which interacts with PGH and helps to reorganize a phosphate-binding part of the active site, is clearly the activation site.

To improve our understanding of the active site in the native form, we have determined the structure of the cadmium-loaded enzyme (Cd-FBPA) crystallized in the presence of CdCl<sub>2</sub>, reasoning that the increase in electronic number from 28 to 46 would assist in clear identification of the transition-metal ion sites. Fortunately, the presence of Cd<sup>2+</sup> improved the quality of the crystals compared with those used by Cooper *et al.* (1996) and we can now include data to 2.0 Å resolution.

## 2. Experimental methods

### 2.1. Crystallization and X-ray data collection

Established protocols (Qamar *et al.*, 1996) provided FBPA with a specific activity of 6.1 U mg<sup>-1</sup>. The enzyme was precipitated with 80% saturated (NH<sub>4</sub>)<sub>2</sub>SO<sub>4</sub>. The precipitate was then dissolved in 50 mM Tris–

HCl, 0.1 M EDTA pH 8.0 and kept at 277 K for 1 h, by which time the specific activity had decreased to 0.04 U mg<sup>-1</sup>. EDTA was removed by gel filtration on a Pharmacia Superdex 200 column previously washed with 0.1 M Tris–HCl, 0.1 M EDTA pH 8.0 and equilibrated with metal-free 0.1 M Tris–HCl pH 8.0. The metal-free state of the column and buffer was maintained by continual passage through a pre-column of iminodiacetic acid chelating resin. The eluted apoenzyme exhibited between 0.5 and 4.0% of the native activity and contained less than 4.0% of the normal Zn<sup>2+</sup> content as measured by atomic absorption spectroscopy. Cd-FBPA was then prepared by addition of 0.3 mM CdCl<sub>2</sub> and the enzyme was dialysed extensively against 50 mM Tris–HCl pH 7.5, 0.3 mM cadmium acetate for 12 h with several changes of buffer. The reconstituted Cd-aldolase had an activity of 1.21 U mg<sup>-1</sup> and, like the native enzyme, was activated by the presence of K<sup>+</sup>, with activities of 5.1 and 20.6 U mg<sup>-1</sup> for Cd-FBPA and Zn-FBPA, respectively.

Batch methods were used to crystallize the enzyme from a 16.5 mg ml<sup>-1</sup> solution in 50 mM Tris–HCl pH 7.5, 3–4% (w/v) PEG 4000, 2 mM CdCl<sub>2</sub>. Hexagonal bipyramidal crystals attained their full size of 0.5 mm in 5–6 d. As we were unable to identify suitable cryoprotection conditions, a single crystal was mounted in a glass capillary and used for data collection on BM14 at the European Synchrotron Radiation Facility, using Fuji image plates as the detector and a custom-made carousel (Brown, 1997; λ = 1.033 Å). Data were processed using *HKL* (Otwinowski & Minor, 1997; Table 1) and were over 94% complete to 2.2 Å; the detector geometry (rectangular plates), the large unit cell *c* dimension and radiation damage accounted for the lower completeness to 2.0 Å. *R* factors for individual images varied from 0.03 to 0.08% and crystal mosaicity increased from 0.08 to 0.16° during data collection.

The crystals are isomorphous with the previously determined hexagonal structure, so this was used as a model (Cooper *et al.*, 1996; PDB code 1zen) truncated to protein residues only; refinement took place using *REFMAC* (Murshudov *et al.*, 1997) and *O* (Jones *et al.*, 1991). The N-terminus and several loop regions of the model had to be rebuilt during refinement. Water molecules and ions were included as refinement progressed. The final model consists of 333 protein residues (residues 1–176, 194–225 and 234–358), five Cd<sup>2+</sup> ions (Cd1–Cd5) and 161 water molecules (statistics are presented in Table 1). The assignment of the five Cd<sup>2+</sup>

**Table 1**

Data quality and refinement statistics.

Values in parentheses are for the outer shell. No resolution or σ cutoff was applied to the data used for refinement.

|   |   |
|---|---|
| Space group                                 | <i>P</i> 6 <sub>1</sub> 22                        |
| Unit-cell parameters (Å)                    | <i>a</i> = <i>b</i> = 77.33,<br><i>c</i> = 290.85 |
| Resolution limits (Å)                       | 38.3–2.0  |
| <i>R</i> <sub>merge</sub>                   | 0.06 (0.29)                                       |
| No. reflections measured                    | 102727  |
| No. unique reflections                      | 31355   |
| Mean <i>I</i> /σ( <i>I</i> )                | 12.8 (1.3)  |
| Completeness (%)                            | 86.9 (51.0)                                       |
| Redundancy                                  | 2.5   |
| No. of protein atoms/water/Cd <sup>2+</sup> | 2538/161/5  |
| <i>R</i> <sub>work</sub>                    | 0.168 (0.25)                                      |
| <i>R</i> <sub>free</sub>                    | 0.193 (0.35)                                      |
| Ramachandran analysis                       |   |
| Allowed (%)                                 | 99.3  |
| Generously allowed (%)                      | 0.7   |
| R.m.s.d. from bond ideality (Å)             | 0.020   |
| R.m.s.d. from angle ideality (°)            | 2.6   |
| Mean <i>B</i> value (Å <sup>2</sup> )       | 25.2  |

ions was based upon careful examination of electron-density omit maps and coordination geometry.

## 3. Results and discussion

The overall structure of Cd-FBPA is similar to previously determined structures. R.m.s.d.s are 0.84 Å for 317 C<sup>α</sup> atoms in common with the hexagonal crystal form, 0.47 Å for 330 C<sup>α</sup> positions in common with the monoclinic form and 0.73 Å for 332 C<sup>α</sup> atoms in common with the FBPA–PGH complex. The discussion will concentrate on the two ions located at the active site. The observed coordination distances are typical of Cd–N and Cd–O bond lengths (Allen *et al.*, 1995) and are given in Table 2.

Cd1 is equivalent to the catalytic Zn<sup>2+</sup> in the PGH complex and to Zn<sub>s</sub> in the monoclinic form (Fig. 2), though with sixfold compared with fivefold coordination. Two of the Cd<sup>2+</sup>-coordinating waters correspond to two PGH O atoms that ligate Zn<sup>2+</sup>. When the activating Na<sup>+</sup> and PGH bind, they cause an ordering of the loop linking strand β6 with helix α8 and this positions His226 to ligate the catalytic Zn<sup>2+</sup> (Hall *et al.*, 1999). In Cd-FBPA this loop is disordered and a water molecule replaces His226 as a ligand.

Cd2 correlates to the structural Zn<sup>2+</sup> in the PGH complex and has tetrahedral coordination, with ligands supplied by two water molecules and the carboxylate side chains of Asp144 and Glu174 (Fig. 2; Table 2). These acidic residues, Asp144 and Glu174, are involved in stabilizing the positions of the histidines that coordinate Cd1 and this feature is shared with FBPA–PGH (Hall *et al.*, 1999). In the FBPA–PGH

**Table 2**  
Metal ion–ligand coordination distances (Å).

Two distances are given where the structures presented two subunits per asymmetric unit.

| Ligands           | Cd <sup>2+</sup> | Zn <sup>2+</sup> in the FBPA–PGH complex | Zn <sub>s</sub> in the monoclinic form |
|-------------------|------------------|--|--|
| Catalytic cation  |                  |  |  |
| His110 NE2        | 2.3              | 2.1, 2.2                                 | 2.1, 2.1                               |
| His264 ND1        | 2.3              | 1.9, 1.9                                 | 2.3, 2.2                               |
| O                 | 2.5 (water)      | 2.2, 2.3 (PGH)                           | 2.4, 2.2 (water)                       |
| O                 | 2.5 (water)      | 2.3, 2.3 (PGH)                           | 2.3, 2.3 (water)                       |
| O                 | 2.4 (water)      | —  | 2.3 (water)                            |
| O                 | 2.6 (water)      | —  | —                                      |
| His226 ND1        |                  | 1.9, 1.9                                 | —                                      |
| Structural cation |                  |  |  |
| Asp144 OD2        | 2.3              | 2.0, 2.0                                 |  |
| Glu174 OE2        | 2.4              | 2.0, 2.1                                 |  |
| O                 | 1.9 (water)      | 1.9, 2.0 (Glu181 OE2)                    |  |
| O                 | 2.2 (water)      | 2.1, 2.1 (water)                         |  |

complex there is an ordering of the loop following strand  $\beta 5$  which places Glu181 in a position to coordinate the structural Zn<sup>2+</sup>. In the structure presented here, the absence of the transition-state mimic in the active site allows greater conformational freedom

of the surface loops, including that containing Glu181, which is replaced by a water ligand.

Analysis of the hexagonal crystal form of Zn-FBPA assigned two metal sites, M1 and M2, as described previously. The Cd-FBPA

structure does not share a metal site with either M1 or M2. Ordered water has been identified at the M1 position, as is the case in the FBPA–PGH complex (not shown). The assignment of NH<sub>4</sub><sup>+</sup> (although K<sup>+</sup> was not discounted) at this position in the monoclinic form was postulated to identify the position of the activating monovalent cation used by FBPA. However, the FBPA–PGH complex clearly identified Na<sup>+</sup> in an alternative position as the activating cation (Hall *et al.*, 1999). The Cd-FBPA structure has an ordered water molecule that corresponds to the M2/Zn<sub>b</sub> site. With the benefit of the high-resolution monoclinic structure to provide guidance, we judge it possible that disorder may also be present in the more weakly diffracting hexagonal crystals of Zn-FBPA and that a water molecule has been modelled where there is in fact a partially occupied Zn<sup>2+</sup> at the catalytic site. When either PGH or Cd<sup>2+</sup> is present there is no ion corresponding to the Zn<sub>b</sub> or M1 site discussed above, suggesting that an ordering of the active site has occurred in the presence of the transition-state mimic or the larger transition-metal ion.

The stability and catalytic activity of Zn-FBPA is significantly enhanced by the presence of millimolar Zn<sup>2+</sup> (von der Osten *et al.*, 1989). We note that in the presence of either millimolar Zn<sup>2+</sup> or Cd<sup>2+</sup>, the structure shows a well ordered cation (structural Zn or Cd<sub>2</sub>; Fig. 2) contributing to the organization of the active site. Two of the remaining three Cd<sup>2+</sup> positions correspond to sites identified as Zn<sup>2+</sup>-coordinating sites in the FBPA–PGH complex (not shown). Cd3 is five-coordinate, interacting with His9 NE21 and His129 ND1 and three water molecules. Cd4 is involved in a bridging interaction between symmetry-related molecules and is coordinated by OE1 and OE2 of Glu246, His256 ND1, Asn27 OD1 and the N-terminus at Ser1. His252 ND1 and two water molecules coordinate the final ion Cd5. These three Cd<sup>2+</sup>-binding sites are all distant from the active site.

#### 4. Conclusions

The first structures of Zn-FBPA presented a confused picture of cation organization in the active site and provided little useful information on metal-ion contributions to the enzyme mechanism. The structure of the FBPA–PGH complex identified the catalytic Zn<sup>2+</sup>, a structural Zn<sup>2+</sup> and a monovalent cation required for maintenance of the active-site architecture. The structure of Cd-FBPA in the hexagonal form, with greatly improved diffraction data, has

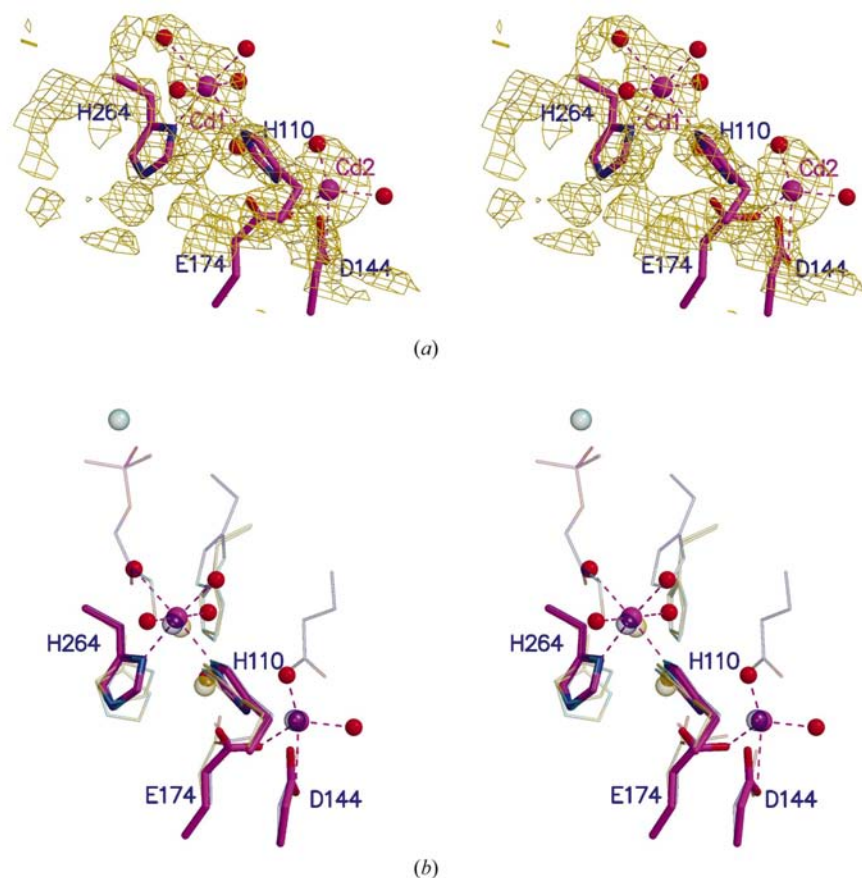


**Figure 2**

The Cd<sup>2+</sup> ions and associated ligands in the active site of Cd-FBPA. (a) Cd<sup>2+</sup> and C atoms are coloured magenta. Water molecules that coordinate Cd<sup>2+</sup> are coloured red and ion–ligand interactions are depicted as red dashed lines. The  $F_o - F_c$  electron-density map is shown as mustard-coloured chicken wire and is contoured at  $3.5\sigma$ . The  $F_c$  terms were calculated without scattering-factor contributions from any atoms within 9 Å of the Cd<sup>2+</sup> sites. (b) The structures of monoclinic Zn-FBPA and FBPA–PGH, slightly modified from Fig. 1, are overlaid for comparison.

confirmed that the two active-site metal ions in the FBPA-PGH structure are also present in the native uncomplexed enzyme, although there are some alterations in the metal-ion coordination. These alterations involve the loss of Glu181 and His226 as ligands for the structural and catalytic metal ions, respectively. The difference may be a consequence of the effect that the substrate analogue and activating ion have in ordering two loops near the enzyme active site.

This work was funded by BBSRC, EPSRC, CCLRC Daresbury Laboratory and The Wellcome Trust. We thank ESRF for access to BM14 and Dr K. Brown for advice.

### References

- Allen, F. H., Kennard, O., Watson, D. G., Brammer, L., Orpen, A. G. & Taylor, R. (1995). *International Tables for Crystallography*, Vol. C, edited by A. J. C. Wilson, ch. 9.5, pp. 685. Dordrecht: Kluwer Academic Publishers.
- Blom, N. S., Tétreault, S., Coulombe, R. & Sygusch, J. (1996). *Nature Struct. Biol.* **3**, 856–862.
- Brown, K. (1997). PhD thesis, University of Loughborough, England.
- Cooper, S. J., Leonard, G. A., McSweeney, S. M., Thompson, A. W., Naismith, J. H., Qamar, S., Plater, A., Berry, A. & Hunter, W. N. (1996). *Structure*, **4**, 1303–1315.
- Gefflaut, T., Blonski, C., Perie, J. & Wilson, M. (1995). *Prog. Biophys. Mol. Biol.* **63**, 301–340.
- Hall, D. R., Leonard, G. A., Reed, C. D., Watt, C. I., Berry, A. & Hunter, W. N. (1999). *J. Mol. Biol.* **287**, 383–394.
- Horecker, B. L., Tsolas, O. & Lai, C. Y. (1972). *The Enzymes*, edited by P. D. Boyer, Vol. 7, pp. 213–258. New York: Academic Press.
- Jones, T. A., Zou, J. Y., Cowan, S. W. & Kjeldgaard, M. (1991). *Acta Cryst.* **A47**, 110–119.
- Kraulis, P. J. (1991). *J. Appl. Cryst.* **24**, 946–950.
- Merritt, E. A. & Murphy, M. E. P. (1994). *Acta Cryst.* **D50**, 869–873.
- Murshudov, N. G., Vagin, A. A. & Dodson, E. J. (1997). *Acta Cryst.* **D53**, 240–255.
- Osten, C. H. von der, Sinskey, A. J., Barbas, C. F., Pederson, R. L., Wang, Y.-F. & Wong, C.-H. (1989). *J. Am. Chem. Soc.* **111**, 3924–3927.
- Otwinowski, Z. & Minor, W. (1997). *Methods Enzymol.* **276**, 307–326.
- Plater, A., Zgiby, S. M., Thomson, G. J., Qamar, S. & Berry, A. (1999). *J. Mol. Biol.* **285**, 843–855.
- Qamar, S., Marshall, K. & Berry, A. (1996). *Protein Sci.* **5**, 154–161.